



## 1. INTRODUCTION

Since the classical investigations by Harlow Shapley (1885-1972), who identified Cepheids and calculated real distances to the globular clusters (GCs) [1], these remarkable objects become the most intensively studied in the Milky Way and in neighboring galaxies. With the launch of the Hubble Space Telescope (HST) it was finally possible to resolve individual stars in their dense central cores. In addition to stars whose presence is expected by the canonical stellar evolution theory, several more exotic objects like blue straggle stars, X-ray binaries, millisecond pulsars, etc., have been indentified in Galactic GCs so far, see e.g. ref. [2].

The GCs play a key role in astrophysics, because they may be considered as large assemblies of coeval stars with a common history, but differing only in their initial masses, although growing evidence for some spread in star formation ages is being collected, see e.g. Piotto, 2010 [3]. The spread of star ages is surely much shorter than the age of the clusters. It is useful here that stars in a GC may be treated statistically with high degree of confidence. Moreover, the number of GCs in the Milky Way is quite large, close to 160. They differ in mass, luminosity, total number of stars, and their spatial densities as a function of distance from the center.

The most fundamental characteristics of the GC such as the total number of stars,  $N$ , and their radial distribution are still poorly known due to their extremely large central densities and slow gradual transition of their peripherals towards the Galactic background. A better knowledge of these characteristics is necessary for a proper estimation of the physical conditions in central parts of GCs. It is particularly interesting to know to what extent their central temperatures differ from the present-day background radiation temperature (2.73K) and what is the temperature gradient across a cluster.

GCs are the oldest objects in the Milky Way galaxy, of the order of  $10^{12}$  years, i.e. large in comparison to a characteristic time-scale over which stars lose memory of their initial orbital conditions. This is a so-called *relaxation time*, of the order of  $10^7$  years according to Chandrasekhar [4]. Therefore, GCs are old enough to attain a dynamic equilibrium and a stable symmetric radial distribution, provided that they were neither significantly disturbed during the last pass through the Galactic disk, nor they collided with other GCs. While the GC-GC collisions are actually rare, it wouldn't be so with the passage through the disk.

The radial distribution of stars is crucial in determining the dynamic properties of a GC, however, this topic is beyond the scope of this study. It is the purpose of this paper to present step-by-step reconstruction of the 3-dimensional radial distributions (3D) of stars in a GC, from the 2-dimensional distributions recorded by telescopes. Our approach is based on the Monte Carlo method

which is applied to various trial functions assumed to be symmetric 3D distributions. The Monte Carlo method allows a fast conversion of the 3D to 2D distribution which is then compared to that observed in the sky.

## 2. THEORETICAL CONSIDERATIONS

We will start the calculations from the assumption of a 3D Gaussian as a trial function for spatial distribution of stars in a GC, because the Gaussian distribution may be considered as a standard radial-symmetric function to which other distributions may be simply compared. The following physical analogy is relevant to the Gaussian distribution function.

The diffusion phenomenon may convert the initial distribution of any particle system to the Gaussian one, generally with time-dependent standard deviation parameter,  $\sigma$ . For example, a droplet of ink immersed inside a large water pool will diffuse continuously, and ink density will attain, due to the chaotic motion of water molecules, a Gaussian distribution with standard deviation increasing proportionally to the square root of time. However, when diffusing particles attract each other, the dispersion parameter,  $\sigma$ , can finally achieve a constant value, just alike in the case of stars distribution in a massive GC. Nonetheless, a low mass cluster will suffer a loss of stars becoming gradually converted to an open cluster, as e.g. M 67 [18].

Deviations of a real distribution from the spatial Gaussian distribution will be considered later on. It is expected, however, that such a deviation will be a rather small correction only to the second and somewhat larger to the fourth central statistical moment, because of rather high spherical symmetry of all the clusters observed in the Milky Way (see McMaster University Catalog [7,8] for eccentricity parameter). Therefore, in the first approximation, the third statistical central moment is zero, and only significant moments remain the second (variance) and the fourth.

Consider a reference frame  $(x, y, z)$  with the origin located in the center of a cluster and the  $z$ -axis oriented outwards a remote observer. The observed distribution of stars in the  $(x, y)$  plane being a small section of the celestial sphere is the projection of their radial 3D distribution. This projection can be obtained from the assumed normal distributions along the three axes. These distributions are defined by a common parameter  $\sigma$ , due to GC symmetry. So, the probability to find a star in the range between  $x$  and  $x + dx$  is given by the following expression:

$$dP_x = \frac{1}{\sqrt{2\pi}\sigma} e^{-\frac{x^2}{2\sigma^2}} dx. \quad (1)$$

Similarly are defined  $dP_y$  and  $dP_z$ , hence the probability to find a star in an infinitesimal box of size  $dx dy dz$  is:

$$dP = dP_x dP_y dP_z = \left(\frac{1}{\sqrt{2\pi}\sigma}\right)^3 e^{-\frac{x^2+y^2+z^2}{2\sigma^2}} dx dy dz. \quad (2)$$

Now we can replace the Cartesian coordinates by the spherical ones nothing that

$$x^2 + y^2 + z^2 = r^2$$

$$dx dy dz \rightarrow dr \cdot r d\theta \cdot r \sin \theta d\varphi.$$

In order to calculate the probability of a star position between spheres of radius  $r$  and  $r + dr$ , we have to integrate the transformed expression (2) over the angular coordinates  $\varphi$  and  $\theta$ :

$$dP_r = \frac{dN_r}{N} = \int_0^{2\pi} d\varphi \int_0^\pi \sin \theta d\theta \cdot \left(\frac{1}{\sqrt{2\pi}\sigma}\right)^3 e^{-\frac{r^2}{2\sigma^2}} dr. \quad (3)$$

The number of stars,  $dN_r$ , between spheres of radius  $r$  and  $r + dr$  is:

$$dN_r = N \sqrt{\frac{2}{\pi}} \frac{r^2 dr}{\sigma^3} e^{-\frac{r^2}{2\sigma^2}}. \quad (4)$$

As it is seen from the above formula  $dN_r$  can be calculated from the total numbers of stars,  $N$ , in a considered cluster and its characteristic radius which is defined by the standard deviation parameter  $\sigma$ . Substituting  $s$  for  $\sqrt{2}\sigma$ , we can easily convert equation (4) to the following equivalent form:

$$\frac{dN_r}{N} = \frac{4}{\sqrt{\pi}} \frac{r^2 dr}{s^3} e^{-\frac{r^2}{s^2}}. \quad (4a)$$

It should be noted at this point that for any spherically symmetric function  $f(r/s)$ , where  $s$  is a characteristic distance parameter, the fraction of stars of the total number  $N$  dispersed between spheres of radius  $r$  and  $r + dr$  may be calculated in similar way:

$$\frac{dN_r}{N} = C \frac{r^2 dr}{s^3} f\left(\frac{r}{s}\right), \quad (5)$$

where  $C = 1/[\int_0^\infty u^2 f(u) du]$  is the normalization constant, and  $u = r/s$ .

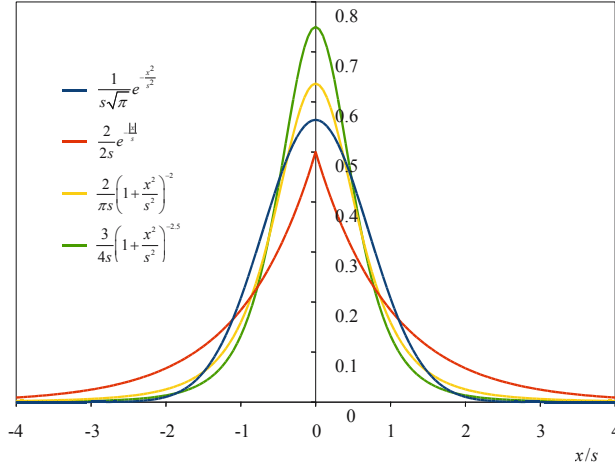


**FIG. 1.** The probability density functions  $f(x) = dP_x/dx$  considered in this study.

In this paper we will consider other spherically symmetric functions as candidates for spatial star distribution around a GC center. Therefore, instead of equation (1) for  $f(x) = dP_x/dx$  we will consider a double exponential function,  $f\left(\frac{x}{s}\right) = \exp(-|x|/s)$ , and the next it will be a squared Cauchy distribution function,  $f\left(\frac{x}{s}\right) = 1/(1+x^2/s^2)^2$ . The first function is also known as the Laplace distribution, whereas the second belongs to the Pearson type VII family probability density functions.

The rationale for using the double exponential function is that the physical conditions in a GC with a massive black hole resemble the electron-proton interaction in the hydrogen atom. The quantum mechanics exactly describes the probability distribution of an electron (radial density) in the lowest energy state by the double exponential function. This function has 4 times larger variance,  $\sigma^2$ , and much larger fourth statistical moment,  $\mu_4$ , than the Gaussian (see Table 1). On the other hand, the squared Cauchy distribution function has a slightly larger variance than the Gaussian, but the fourth statistical moment is infinite, therefore it may be a better candidate for describing a broad star distribution in GCs. Actually the squared Cauchy function nicely resembles a Gaussian, except that it has a larger overall dispersion. These normalized functions are shown in Fig. 1 and their statistical properties are collected in Table 1. All the functions listed in Table 1 will be used below as trial functions for their converting to 2D radial densities.

**TABLE 1.** Statistical properties of the normalized distribution functions  $f(x)$  considered in this study,  $\sigma^2$  is the variance and  $\mu_4$  is the 4-th statistical moment, which are defined as  $2\int_0^\infty x^2 f(x)dx$  and  $2\int_0^\infty x^4 f(x)dx$ , respectively, where  $x = r/s$ .

| <i>Function</i>   | <i>Name</i>                           | $\sigma^2$               | $\mu_4$          |
|---|---------------------------------------|--------------------------|------------------|
| $\frac{1}{\sqrt{\pi}s} e^{-\frac{x^2}{s^2}}$            | Normal or Gaussian                    | $\frac{s^2}{2}$          | $\frac{3}{2}s^4$ |
| $\frac{1}{2s} e^{-\frac{ x }{s}}$                       | Double-exponential                    | $2s^2$                   | $24s^4$          |
| $\frac{2}{\pi s} \left(1 + \frac{x^2}{s^2}\right)^{-2}$ | Squared Cauchy                        | $s^2$                    | $\infty$         |
| $\frac{3}{4s} \left(1 + \frac{x^2}{s^2}\right)^{-2.5}$  | Pearson type VII                      | $\frac{s^2}{2}$          | $\infty$         |
| $C(s,m) \cdot \left(1 + \frac{x^2}{s^2}\right)^{-m}$    | Power law or generalized Schuster law | $< \infty$ , for $m > 2$ | $\infty$         |

The squared Cauchy distribution function is a slightly modified function  $f\left(\frac{r}{s}\right) = 1/(1+r^2/s^2)^{2.5}$ , which is known from archival literature (Plummer 1911 and Dicke 1939) listed as refs [5, 6]. This function has been obtained as one of elementary functions found within the solutions of the Emden's polytropic gas sphere equation

$$\frac{d}{dr} \left( \frac{r^2}{\rho} \frac{d\rho^\gamma}{dr} \right) + b^2 \rho r^2 = 0, \quad (6)$$

where  $\rho$  is the gas density,  $r$  is radial distance,  $\gamma$  is the ratio of specific heats of the gas, and  $b$  is a parameter. The above mentioned function  $1/(1+r^2/s^2)^{2.5}$  is strictly relevant for  $\gamma = 1.2$  only, whereas atomic and molecular hydrogen has  $\gamma$  value 1.67 and 1.40, respectively. Hence the squared Cauchy function has rather statistical rationale only, and it is not intimately related to the conditions of early gas nebula from which the cluster was formed as it was proposed by Plummer.

Yet more general equation for radial distribution of stars in globular clusters is alike double Cauchy distribution, but with power treated as an adjustable parameter. This type of radial distribution is known as the ‘‘power law’’ or generalized Schuster law and it was considered by Živkov and Ninkovic [11] as a simple formula for replacement of the King's radial distribution in spherical stellar systems.

### 3. NUMERICAL CALCULATIONS

In the next step we have to project the assumed 3D distributions onto the  $x, y$  plane, in order to compare the obtained 2D distributions with that recorded by telescopes.

For numerical conversion of any 3D radial distribution to 2D we will apply the Monte Carlo method. The algorithm developed for this purpose initially divides the space around the center of a GC into concentric spheres. The first sphere has radius  $\Delta r$ , whilst the radii of the subsequent spheres are increased by  $\Delta r$ . The number of stars  $\Delta N_r$ , between two neighboring spheres, indexed by  $n$  and  $n+1$ , is calculated from equation (5) for  $r = r_n + \frac{1}{2} \Delta r$ . For each star of the sub-set of  $\Delta N_r$ , the spherical coordinates  $r$  and  $\varphi$  are randomly drawn from the intervals  $(r_n, r_n + \Delta r)$  and  $(0, 2\pi)$ , respectively. The coordinate  $\theta$  was calculated from  $\arcsin(\theta)$  function, the values of which were randomly drawn from the interval  $(-1, 1)$ . The described procedure creates a uniform star distribution within the each sphere.

In the last step of the numerical procedure the Cartesian coordinates  $(x, y, z)$  of all the stars are calculated from the obtained  $(r, \varphi, \theta)$  coordinates. The projection of the stars onto the planar surface  $x, y$  is made by setting  $z = 0$  for all the  $N$  stars. From the obtained planar distribution of stars, a 2D radial density function is calculated (i.e. GC profile) which is then compared to observations. We adjust the parameters  $C, s$  and  $m$  in order to obtain the best agreement of the plotted profile with that taken from ref. [9] using as a criterion the lowest value of root-mean-square deviation. The sum of stars drawn in the simulation at optimum distribution parameters is treated as the total number of stars,  $N$ .

Normalized radial distribution functions of stars in 3D space, which were considered in this paper are listed in Table 2.

**TABLE 2.** Normalized radial distribution functions applied in this study.

| <i>Name</i>        | <i>Radial distribution function</i>                                      |
|--------------------|--|
| Normal or Gaussian | $\frac{4}{\sqrt{\pi}} \frac{r^2}{s^3} e^{-\frac{r^2}{s^2}} dr$           |
| Double-exponential | $\frac{1}{2} \frac{r^2}{s^3} e^{-\frac{r}{s}} dr$                        |
| Squared Cauchy     | $\frac{4}{\pi} \frac{r^2}{s^3} \left(1 + \frac{r^2}{s^2}\right)^{-2} dr$ |
| Pearson type VII   | $3 \frac{r^2}{s^3} \left(1 + \frac{r^2}{s^2}\right)^{-2.5} dr$           |

## 4. RESULTS AND DISCUSSION

In Fig. 2a we show the 2D star distribution in the  $x,y$  plane generated for  $N = 7 \cdot 10^4$  stars distributed in 3D space according to the squared Cauchy radial function. This figure shows the simulated stars distribution in the M 13 (NGC 6205) globular cluster, the photo of which is shown in Fig. 2b for comparison. A certain amount of eccentricity is seen in the photo of M 13. According to the catalog data in refs. [7,8] M 13 has an absolute magnitude  $-8.55^M$ , core radius 0.62 arc min, and half-light radius 1.69 arc min, the eccentricity  $1 - b/a = 0.1$ , where  $a$  and  $b$  are axes of the ellipse overlapping the cluster core.

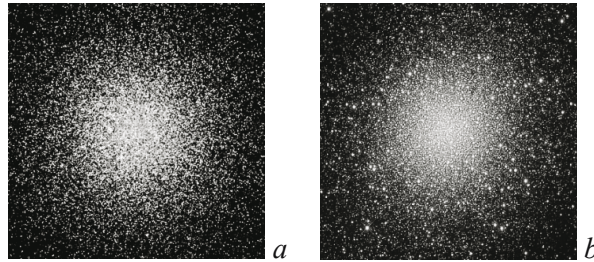


**FIG. 2.** *a.* The stars distribution in M13 cluster simulated by the Monte Carlo method, while *b* is a photo of this GC for comparison, source: <http://www.osservatoriomtm.it>

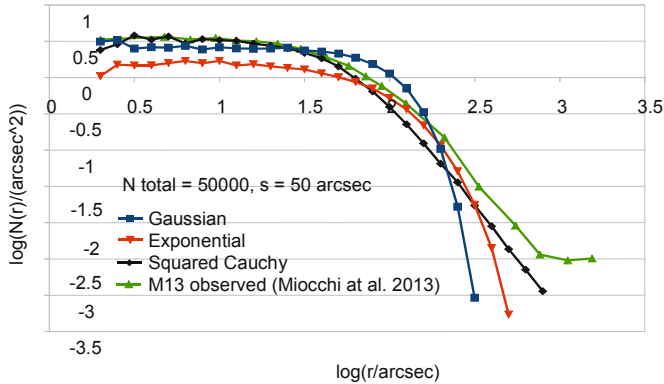


**FIG. 3.** The comparison of 2D distribution of stars in modeled M 13 cluster using 3 different trial functions for 3D radial distribution having identical characteristic size parameter,  $s$  (the disagreement with the outermost 3 points of the M13 profile is due to the nearly constant 2D density superimposed profile of the Galactic stellar background). Each function was normalized for the total number of stars  $N = 50,000$ . The obtained distributions are compared with the observed distribution by Miocchi et al. [9]. It is seen that using the squared Cauchy function will lead to a better agreement for assumed larger number of stars and size parameter.

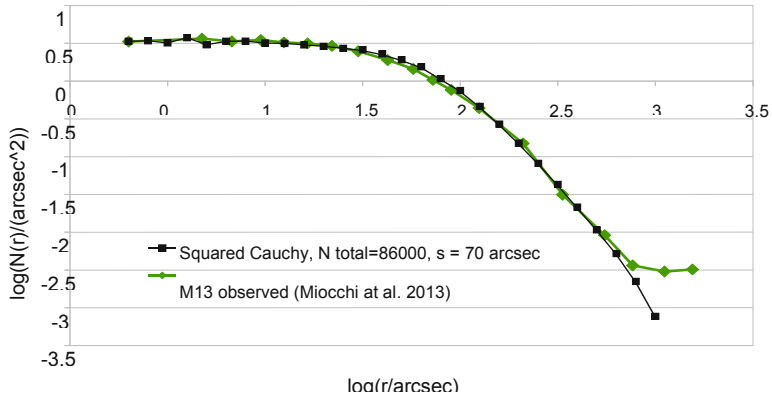


**FIG. 4.** The comparison of the converted 3D distribution, which is normalized squared Cauchy function  $1/(1+r^2/s^2)^2$  with the observed 2D profile [9] for assumed larger number of stars and optimally adjusted  $s$  value. The obtained 2D distribution fully agrees with the observed profile of M 13 cluster.

Fig. 3 shows the profiles of the projected distributions of stars into  $x,y$  plane for  $N = 5 \cdot 10^4$  stars with the same size parameter,  $s$ , of the following 3D radial distributions: (i) Gaussian, (ii) double exponential, and (iii) squared Cauchy. All these functions were normalized by an appropriate multiplier  $C$  to obtain the same total number of stars ( $N = 5 \cdot 10^4$ ) and all of them have identical dimensional parameter  $s = 50$  arcsec.

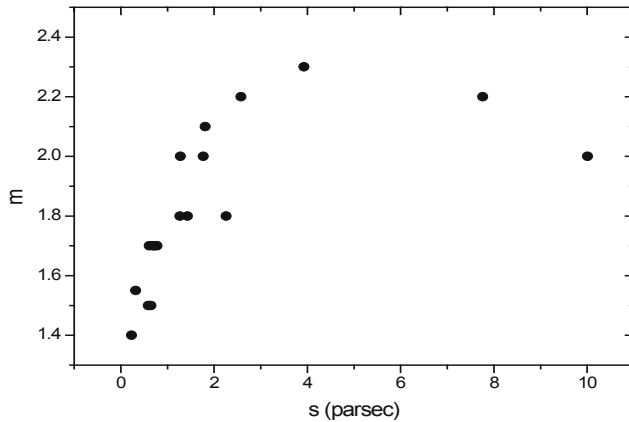


**FIG. 5.** The empirical relationship between the size parameter  $s$  in parsecs of a GC and the power factor  $m$  determining the slope of the observed profile. It is seen that the larger the core with respect to the overall system size, the smaller the radial extent of the outer "envelope" region and vice versa.

Although the obtained plots resemble a real-world observed star distribution in M 13, which is plotted as green line in Fig. 3 using data from recent study by Miocchi et al. [9], neither of them fits well to the observed distribution. The best fit is obtained with the squared Cauchy distribution, where by varying its  $s$  parameter we can finally achieve excellent agreement with the observed distribution, as shown in Fig. 4.

**TABLE 3.** Results of numerical simulation of 3D star distributions in GCs for those star counting profiles were available (Miocchi et al. [9]). The distance was taken from [8] whereas  $C$ ,  $m$ , and  $s$  are parameters of formula (9) were found by the Monte Carlo method as optimal. The total number of stars,  $N$ , is calculated from the fitted 3D distribution by counting the stars drawn in the simulation.

| NGC  | Distance<br>[kpc] | $C$    | $N$    | $m$  | $s$ [arcsec] | $s$ [pc] |
|------|-------------------|--------|--------|------|--------------|----------|
| 104  | 4.5               | 0.21   | 147100 | 1.5  | 30           | 0.65     |
| 1851 | 12.1              | 0.0025 | 4400   | 1.4  | 4            | 0.23     |
| 1904 | 12.9              | 0.019  | 6400   | 1.7  | 11           | 0.69     |
| 2419 | 82.6              | 0.16   | 11700  | 2    | 25           | 10.01    |
| 5024 | 17.9              | 0.07   | 17100  | 1.8  | 26           | 2.26     |
| 5139 | 5.2               | 0.26   | 104100 | 1.5  | 200          | 5.04     |
| 5272 | 10.2              | 0.17   | 20900  | 1.8  | 29           | 1.43     |
| 5466 | 16                | 0.1    | 4500   | 2.2  | 100          | 7.76     |
| 5824 | 32.1              | 0.012  | 1900   | 1.7  | 5            | 0.78     |
| 5904 | 7.5               | 0.28   | 35000  | 1.8  | 35           | 1.27     |
| 6121 | 2.2               | 0.04   | 13300  | 1.5  | 55           | 0.59     |
| 6205 | 7.1               | 1.75   | 89400  | 2.2  | 75           | 2.58     |
| 6229 | 30.5              | 0.054  | 3900   | 2    | 12           | 1.77     |
| 6254 | 4.4               | 0.12   | 8300   | 2    | 60           | 1.28     |
| 6266 | 6.8               | 1.4    | 156000 | 2.1  | 55           | 1.81     |
| 6341 | 8.3               | 0.025  | 7300   | 1.7  | 18           | 0.72     |
| 6626 | 5.5               | 0.01   | 5400   | 1.55 | 12           | 0.32     |
| 6809 | 5.4               | 0.18   | 13300  | 2.3  | 150          | 3.93     |
| 6864 | 20.9              | 0.021  | 6700   | 1.7  | 6            | 0.61     |

Although the proposed star distribution in GCs (i.e. squared Cauchy) is not directly related to the dynamics of the system, it seems to be not far from those based on mechanical principles [17]. Actually the squared Cauchy radial function was considered by us to be more appropriate than Cauchy distribution function which has infinite variance or standard deviation, whereas the squared Cau-

chy function has a finite standard deviation. Through its larger dispersion in comparison to Gaussian or exponential function it appears to be most appropriate of 3D star distribution in M 13 (Figs 3 and 4).

However, often the best fit to the observed profiles leads to the “power law” function or Schuster density law [10-12], where the power  $m$  varies from 1.4 to 2.3 as it is shown in Fig. 5. Studying a sample of Milky Way GCs for which star counting profiles have been published recently [9], we have noticed an interesting non-linear correlation between parameters  $s$  and  $m$  (Fig. 5).

In this way by using the Monte Carlo approach we have confirmed a great significance of power-law distribution function. Though the power-law is considered in literature as *ad hoc* fitting function [13], in most cases it better fits to the observation data than King and Wilson models [14]. The major weakness of this function over the King model is that it is not dynamically self-consistent in the sense that it produces a dynamical equilibrium. However, for the purposes of this study the power-law radial distribution is fully sufficient, because we do not consider star velocities, but their spatial distribution only.

## 5. RADIATION TEMPERATURE ACROSS GCS

We can now use the Monte Carlo approach to estimate the radiation temperature across a GC.

Let us assume for this purpose that each star of a GC produces the same amount of electromagnetic radiation flux of 1366 W/m<sup>2</sup> (solar constant) at the distance of one astronomical unit. According to this simplified assumption the radiation flux density from a star at distance  $r_i$  from a fixed point in the free space of GC can be calculated, using formula:

$$\Phi_i = \frac{1366 \text{ W/m}^2}{(r_i / 1 \text{ AU})^2} \quad (7)$$

The total irradiation flux density  $\Phi$  at this point is  $\sum_i^N \Phi_i$ , where  $N$  is total number of stars in the considered GC. The total flux density  $\Phi$  of electromagnetic radiation determines the temperature  $T$  of black body, which fully absorbs this radiation. The relation between  $\Phi$  and  $T$  is described by the Stefan–Boltzmann law

$$\Phi = \sigma T^4, \quad (8)$$

where  $\sigma$  in formula (8) is the Stefan–Boltzmann constant. Using the above two equations, we can calculate approximately the radiation temperature in the space

inside a modeled GC (by the Monte Carlo method) as a function of distance from its center. Two examples of such temperature profiles are shown in Fig. 6.

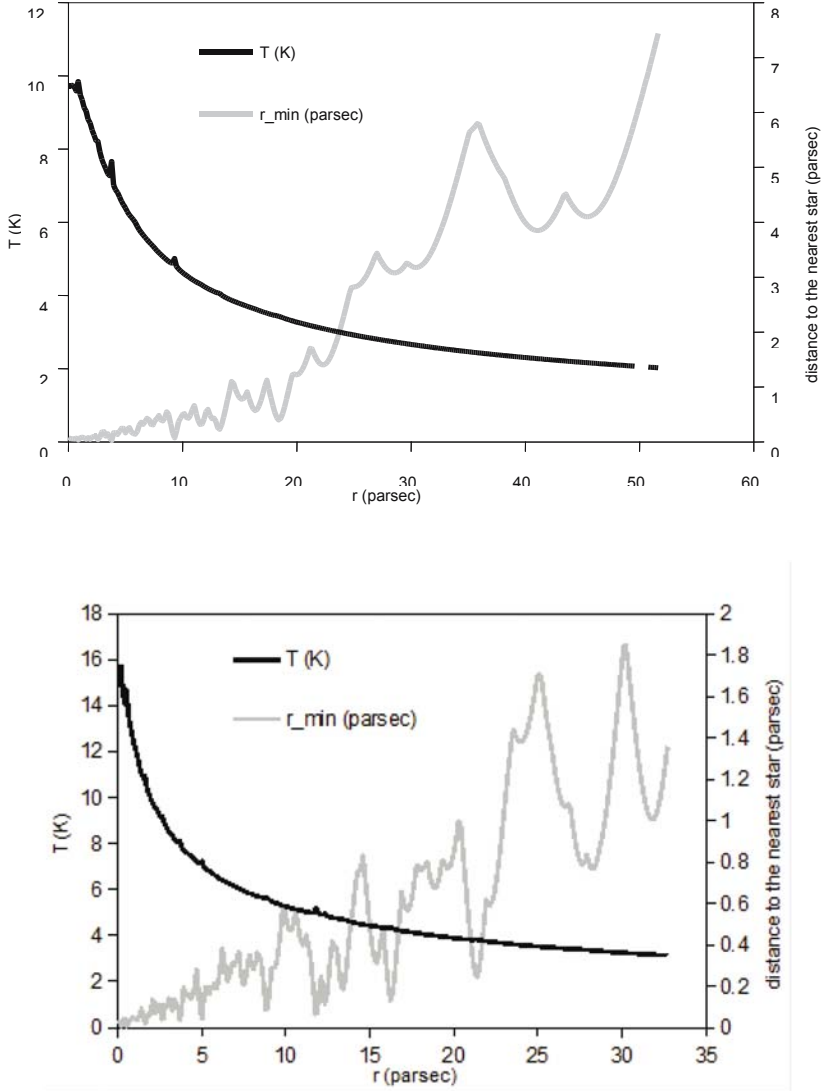


**FIG. 6.** Radiation temperatures (above background of 2.7 K) as a function of distance from the center of modeled M13 and 47 Tucane clusters (black lines). The spikes in black lines are due to proximity to the nearest star, the distances of which are plotted as gray lines.

## 6. CONCLUSIONS

A critical discussion of the calculations presented above leads to a conclusion that 3D radial density of stars is well described by two-parameters function known as the power-law distribution or generalized Schuster density law:

$$f(r) = C \left( 1 + \frac{r^2}{s^2} \right)^{-m}, \quad (9)$$

where  $C$  is the normalization constant,  $s$  is the size parameter and  $m$  is related to the observed slope of the star density profile.

With this function we have calculated present-day radial temperature distribution in the free space inside two GCs: M 13 and 47 Tucane. The last one, being one of the largest Milky Way cluster, has the central radiation temperature of  $\sim 16$  K above the present-day Universe background temperature (2.7 K). Though temperatures across GCs are meaningless in the astrophysical modeling of stars evolution, however we suppose that the temperature gradient plays a great role of a ‘‘mop’’ which cleans the vacuum inside the GCs. Thanks to its action and perhaps some gas accretion by white dwarfs, we have an ideal insight into the interiors of GCs by the HST. Recent density determination of ionized gas (probably the dominant component of the intra-cluster medium) by radio-astronomical observations of 15 pulsars in 47 Tucane yields  $0.067 \pm 0.015 \text{ cm}^{-3}$  only [16]. This is about 100 times the free electron density of the interstellar medium in the vicinity of this GC. Such a low density is undetectable by other methods.

## ACKNOWLEDGEMENTS

The authors wish to express their gratitude to Dr. Paolo Mocchi from the Department of Physics and Astronomy, University of Bologna, Italy, for comments on the manuscript and help in access to recent literature. We are grateful to Dr. Tomasz Durakiewicz from Los Alamos National Laboratory for corrections of English.

## REFERENCES

1. Struve O. and Zebergs V. (1962) *Astronomy of the 20<sup>th</sup> Century*, Macmillan Co.
2. Ferraro F.R., *Exotic Populations in Galactic Globular Clusters*, in: *The Impact of HST on European Astronomy, Astrophysics and Space Science Proceedings*, Springer Science + Business Media B.V., 2010, p. 51.
3. Piotto, G., 2010. *Observational Evidence of Multiple Stellar Populations in Star Clusters*, PKAS 25, 91.

4. Chandrasekhar S. (1960) *Principles of Stellar Dynamics*, Dover, New York.
5. Plummer H.C. (1911). *On the problem of distribution in globular stars clusters*, Monthly Notes LXXI, **5**, 460-470.
6. Dicke R. H. (1939) *The radial distribution in globular clusters*, Astronomical J. **1111**, 108-110.
7. *Catalogue of Milky Way Globular Cluster Parameters*, <http://www.physics.mcmaster.ca/Globular.html>
8. *Catalog of Parameters for Milky Way Globular Clusters: The Database Compiled by William E. Harris*, McMaster University, This revision: December 2010 <http://physwww.physics.mcmaster.ca/~harris/mwgc.dat>
9. Miocchi P., Lanzoni B., Ferraro F. R., Dalessandro E., Vesperini E., Pasquato M., Beccari G., Palla C., and Sanna N. (2013) *Star count density profiles and structural parameters of 26 galactic globular clusters*, The Astrophysical Journal, **774**, 151 (16pp).
10. Ninković S. (1998) *On the generalized Schuster density law*, Serbian Astronomical Journal **158**, 15-21.
11. Živkov, V. and Ninkovic, S. (1998) *On the generalized Schuster density law and King's formula*, Serbian Astronomical Journal **158**, 7-11.
12. Von Lohmann W. (1964) *Dichtegesetze und mittlere Sterngeschwindigkeiten in Sternhaufen*, Z. Astrophys. **60**, 43-56.
13. McLaughlin Dean E. and van der Marel Roeland P., *Resolved massive star clusters in the Milky Way and its satellites: brightness profiles and a catalog of fundamental parameters*, The Astrophysical Journal Supplement Series **161**, 304–360, December 2005.
14. Elson R. A. W., Fall S. M. and Freeman K. C. (1987) *The structure of young star clusters in the Large Magellanic Cloud*, The Astrophysical Journal **323**, 54-78.
15. Diederik Kruijssen J. M., Mieske S.. *The mass-to-light ratios of Galactic Globular Clusters*. To appear in the proceedings of "Galaxy Wars: Stellar Populations and Star Formation in Interacting Galaxies" (Tennessee, July 2009), arXiv:0910.4773
16. Freire P. C., Kramer M., Lyne A. G., Camilo F., Manchester R. N., D'Amico N. (2001) *Detection of ionized gas in the globular cluster 47 Tucanae*, The Astrophysical Journal **557**, L105-L108.
17. King, I., R. (1966) *The structure of star clusters. III. Some simple dynamical models*, Astronomical Journal **71**, 64-75.
18. Naim S., Griv E. (2012) *Examining the M67 classification as an open cluster*, IJAA **2**:167-173.